Applied Catalysis B: Environmental 181 (2016) 747–753

Contents lists available at ScienceDirect

Applied Catalysis B: Environmental

journal homepage: www.elsevier.com/locate/apcatb

Reductive dechlorination in water: Interplay of sorption and reactivity

Frank-Dieter Kopinke[a,*], Gunther Speichert[a,b], Katrin Mackenzie[a], Evamarie Hey-Hawkins[b]

[a] Department of Environmental Engineering, Helmholtz Centre for Environmental Research—UFZ, Permoserstrasse 15, D-04318 Leipzig, Germany
[b] Institute of Inorganic Chemistry, Faculty of Chemistry and Mineralogy, University Leipzig, Johannisallee 29, D-04103 Leipzig, Germany

ARTICLE INFO

Article history:
Received 1 June 2015
Received in revised form 11 August 2015
Accepted 14 August 2015
Available online 20 August 2015

Keywords:
Dechlorination
Zero-valent iron
Activated carbon
Carbo-Iron
Sorption
Spillover

ABSTRACT

Trichloroethene (TCE) dechlorination by nanoscale zero-valent iron (nZVI) in aqueous suspension was investigated in absence and presence of microscale activated carbon (AC). The TCE adsorbed within the AC micropores is available to dechlorination, although a direct contact between sorbed TCE and nZVI is ruled out. The AC functions as a mediator of redox equivalents between the external reductant and the internal sorbate. Therefore, AC plays the role of an adsorbent as well as a dechlorination catalyst driven by the reductive power of nZVI. The dechlorination product patterns in the AC–nZVI mixture and the AC-free slurry are similar, yielding ethane, ethene and ethyne as primary products. One can interpret this as spillover-like transport of mobile reactive species from the iron surface via the carbon matrix to the sorbate. In order to distinguish between transported electrons or hydrogen species, electrochemical experiments with and without the generation of nascent hydrogen (H*) were conducted. They prove the significant role of reactive hydrogen in the nZVI–AC system and favour the spillover mechanism. Ethyne and *cis*-DCE are the dominant products from TCE in the absence of H* species, whereas total dechlorination and hydrogenation occurred in the presence of H*, yielding ethane and ethene as the dominant primary products. The observed interplay between sorptive enrichment and chemical degradation of pollutants inside the AC pores may offer options for improved iron-carbon composite materials and reactor designs.

1. Introduction

Since its first introduction by Gillham and O'Hannesin in the early 1990s [1,2] as a powerful reducing agent for environmental remediation, iron has been extensively studied and its performance has been improved by a variety of measures [3]. One of the most promising enhancements is nano-scale ZVI (nZVI), introduced in the late 1990s [4–14]. Notwithstanding its versatile capabilities, ZVI has some significant limitations which constrain its efficiency, e.g. its low affinity to hydrophobic organic compounds such as chlorinated hydrocarbons [15–18]. These belong, however, to the most widespread groundwater pollutants. Due to their usually low concentrations in contaminated environmental compartments (μg/L to mg/L range) it is desirable to enrich them in the close vicinity of the reactive iron centres. This is the basic idea behind the development of carbon-iron composite materials [19–31] such as Carbo-Iron™ [32–36]: activated carbon (AC) colloids collect hydrophobic pollutants from the aqueous phase, which can then be reductively degraded by nZVI deposited on and inside the porous carbon matrix. Carbo-Iron as an emerging remediation reagent is currently undergoing field testing [37,38]. Kinetic and mechanistic evaluations of the performance of the Carbo-Iron composite indicate a beneficial interplay between sorptive enrichment and chemical reactivity of substrates [39]. One can speculate that this interplay is based on a sufficiently high mobility of the substrates across the sorbent surface such that they can move to the reactive iron centres.

Recently, the group of Tang et al. [40] demonstrated that significant reduction of trichloroethene (TCE) – sequestered in AC micropores – can take place, even though direct contact with the reductant nZVI was impossible. The authors proposed that AC serves as the conductor for the transfer of electrons or atomic hydrogen from nZVI to the micropores of the AC wherein adsorbed TCE molecules (0.02 wt%) are degraded. Although the way the experiments were conducted in their study did not allow a full clarification of the findings, they give clear evidence of the chemical reactivity of TCE adsorbed in AC pores.

Oh et al. [41,42] were able to show that graphite is not only an electron conductor, transferring electrons from ZVI to reactive sorption sites, but is also capable of channelling reactive hydrogen

* Corresponding author. Fax: +49 341 235 451234.
E-mail address: frank-dieter.kopinke@ufz.de (F.-D. Kopinke).

http://dx.doi.org/10.1016/j.apcatb.2015.08.031
0926-3373/

species, most likely H atoms. Due to the applied experimental design (dialysis cells with thin graphite membranes, 140–380 μm thick) they could measure the mobility of H/D-species within the bulk graphite, which was in the order of 10^2 μm/h.

In contrast to these findings, other studies led to the conclusion that graphite as a common constituent of commercial cast iron does not mediate reduction of chlorinated ethenes, but rather acts as a nonreactive sink where the substrate molecules are protected from reduction [15–18].

The aim of the present study is to re-inspect the interaction of nZVI and AC for degradation of chlorinated hydrocarbons in aqueous suspension. Due to the strong sorption of the substrate TCE within the microporous carbon matrix, the degradation process has to proceed via a solid–solid interaction, possibly by spillover of reactive species between the involved particle types.

2. Materials and methods

2.1. Chemicals and reagents

Pulverised AC was purchased from Norit Nederland B.V. (type SX1, S_{BET} = 900 m^2/g, particle size 3–10 μm measured in suspension by optical microscopy) and used as received. As AC cloth, FC1001 from Actitex, France, $S_{BET} \approx 1000\ m^2/g$, was used. TCE (99.5%), Na_2CO_3 p.a. and Na_2SO_4 p.a. were from Aldrich. Ultrapure water (Millipore Simplicity 185, 18.2 MΩ cm) was used for the preparation of all aqueous solutions. Microiron particles (μZVI, $d_p \approx 5$ μm) were purchased from Merck (Fe^0 content >98 wt%). The nZVI used, designated as RNIP (reactive nanoscale iron particles) in the respective literature and supplied by Toda Kogyo Corp., Japan, was in the form of dry particles. The Fe^0 content of the RNIP was (21.9 ± 0.4) wt%, determined by means of acidic digestion with HCl (18%) followed by H_2 quantification via GC-TCD analysis (details see SI). Its specific surface area was about 24 m^2/g (N_2 adsorption at 77 K, BET isotherm).

2.2. Kinetic experiments

All experiments were conducted in 250 mL glass bottles equipped with Mininert™ valves made from PTFE. 160 mL of degassed 0.2 M $NaHCO_3$ solution was filled into a bottle, purged with argon before 0.8 g RNIP was added under inert conditions, yielding an initial RNIP concentration of about 5 g/L (1.1 g/L Fe^0). The suspensions were sonicated for 30 min in an ultrasonic bath to achieve particle disaggregation. TCE and benzene stock solutions (in methanol) were injected into the suspensions, giving initial TCE and benzene concentrations of 6 mg/L and 0.2 mg/L, respectively. 100 μL methane was injected into the headspace, resulting in a methane concentration of 0.11 vol%. Benzene and methane served as internal standards for GC analyses (see remarks in Supplementary information). Experiments in the absence of AC are named benchmark experiments, since they exclusively reflect the reactivity of RNIP. For experiments in the presence of AC, 160 mg of dry AC powder was suspended in 80 mL of the bicarbonate solution under inert conditions and sonicated for 30 min before TCE was added. The suspension was shaken at 120 rpm for two weeks in order to approach sorption equilibrium of TCE on AC (no significant change of its headspace concentration). The RNIP suspension (0.8 g in 80 mL bicarbonate solution) was freshly prepared according to the protocol above, then transferred via a cannula to the AC suspension. The final AC concentration was 1 g/L. The other initial concentrations were the same as for the benchmark experiments.

For each kinetics experiment, four identical bottles were prepared and horizontally shaken at 120 rpm at ambient temperature (T = 22 ± 2 °C) for the entire reaction period. In order to trace educt and product concentrations, a number of headspace and liquid samples were withdrawn during the reaction time and analysed as described below.

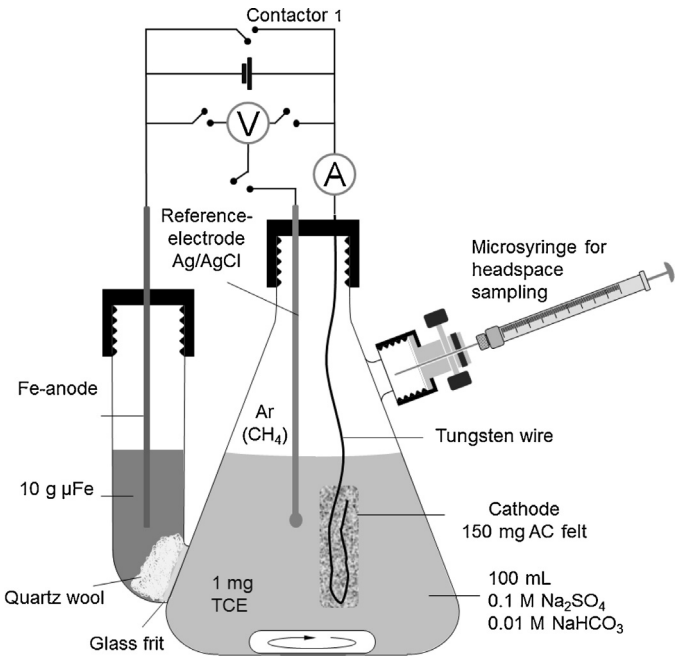

Fig. 1. Schematic presentation of the electrochemical cell for dechlorination experiments.

In the batch experiments, 200 mM bicarbonate solution was chosen as background electrolyte. Due to its low buffer capacity in the lower alkaline pH range, the pH increased slightly during the reaction periods (e.g. from 8.7 to 9.2 within 200 h in the absence of AC and from 9.0 to 9.8 within 1600 h in the presence of AC). Established buffer systems appeared to be less appropriate because of significant interactions with either ZVI or AC (see Supplementary information).

2.3. Electrochemical experiments

The electrochemical cell used is shown in Fig. 1 and consists of a 2-compartment glass body with Mininert™ valve for headspace and liquid sampling. The anode compartment was filled with μZVI and contacted by means of an iron bar (d_{bar} = 3 mm). The cathode compartment contained a piece of felt-like AC cloth (60 × 20 mm, 150 mg). Both compartments were separated by a glass frit but electrically connected, either directly or via an external DC source (Power Supply EA-PS 7032-100, Electro-Automatic GmbH, Germany).

The catholyte (100 mL 0.1 M Na_2SO_4 + 0.01 M $NaHCO_3$, pH 8.5 ± 0.3) was continuously mixed by a magnetic stirrer. The cathode potential was measured against an Ag/AgCl reference electrode (3 M, $E^{25\,°C}$ = +222 mV vs. SHE, Schott, Germany). After purging the cell with Ar and adding 1 mg of TCE and 100 μL of methane (as internal GC standard) in the cathode compartment, the system was allowed to approach to sorption equilibrium for >24 h.

2.4. Analytical methods

Gas samples (25 μL) were taken from the headspace over the reaction slurries and analysed by means of common GC methods for methane, ethyne, ethene, and ethane (polystyrene–divinylbenzene HP-PLOT Q capillary column 30 m × 0.53 mm from Agilent and DB-1 capillary column 50 m × 0.32 mm × 5 μm, FID) as well as for TCE

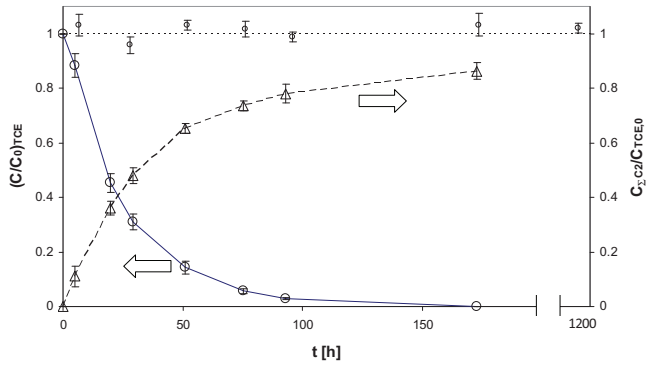

Fig. 2. Kinetics of the dechlorination of TCE with nZVI in aqueous suspension ($C_{TCE,0}$ = 6 mg/L, C_{nZVI} = 5 g/L, 200 mM $NaHCO_3$, pH 8.7–9.2, T = 22 ± 2 °C): ○ = $(C/C_0)_{TCE}$ in the benchmark experiment, o = in the blank run without nZVI, both from GC–MS headspace analyses, △ = $C_{\Sigma C2}/C_{TCE,0}$ from GC-FID headspace analyses; application of combined internal (methane) and external (ethane) calibration. Error bars represent one standard deviation of single values from the mean value out of 4 replicate experiments.

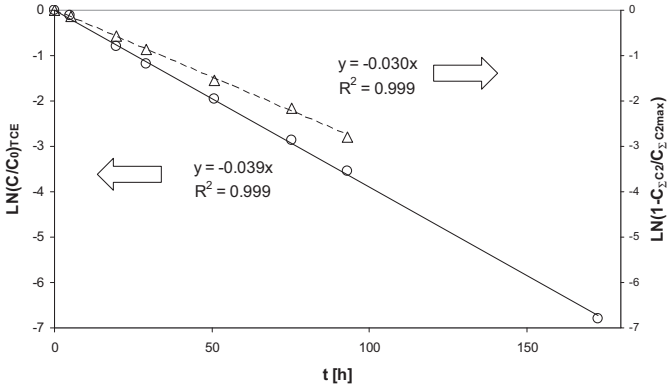

Fig. 3. Kinetics of the dechlorination of TCE with nZVI in aqueous suspension: regression of data (and symbols) from Fig. 2 according to first-order reaction kinetics. C_2-product formation is normalised to a constant reaction selectivity of $C_{\Sigma C2,max}/C_{0,TCE}$ = 0.85.

and benzene (HP-5MS capillary column 30 m × 0.32 mm × 0.25 μm, MS detection) using a Shimadzu GC–MS QP 2010.

In the presence of AC it is more difficult to quantify headspace analyses of strongly sorbing components. Therefore, aliquots of the reaction slurry were taken and subjected to exhaustive solvent extraction according to the following protocol: 1 mL aliquot of the suspension was withdrawn and exchanged with 1 mL of fresh electrolyte solution in order to maintain a constant volume in the reaction bottles. The sample was alkalised with 0.5 mL of 1 M NaOH in order to inhibit further reaction and extracted with 1 mL of toluene (containing 1 mg/L of benzene as internal standard) for 24 h under continuous shaking. After phase separation and filtration of the toluene extract through a 0.2 μm syringe filter, 1 μL of the extract was analysed by means of GC–MS. The extraction recovery of TCE was determined to be about (90 ± 5)%. The GC–MS analyses of extracts offer the opportunity to look for reaction products. No significant concentrations of partially dechlorinated intermediates such as vinyl chloride and dichloroethenes were detected for the batch experiments.

3. Results and discussion

3.1. Dechlorination with RNIP only

The dechlorination kinetics for TCE is presented in Figs. 2 and 3, as course of concentrations and in semi-logarithmic coordinates, respectively. The data points are mean values resulting from four independent experiments under identical conditions. Error bars reflect one standard deviation of single replicates.

The very broad linear range in Fig. 3 up to a TCE conversion of 99.9% indicates a clear first-order kinetics. Hence, it is not necessary to consider a Langmuir–Hinshelwood kinetics with partial site saturation [43–45] under the applied reaction conditions (C_{TCE} = 6. . .0.006 mg/L). This finding is in accordance with the results of Liu et al., who concluded that there is an abundance of reactive sites on the RNIP surface and that factors other than TCE competitive sorption (at $C_{0,TCE}$ = 35 μM and 2200 μM) control the reaction rates [46]. In another study [47] it was explicitly proved that the TCE rate constant was unaffected by its concentration up to at least 460 μM (60 mg/L). Note that a clear first-order reaction kinetics with respect to the TCE concentration is an essential pre-condition for the conclusions to be drawn in the present study. Due to the large stoichiometric surplus of ZVI (20 mM) in relation to TCE (45 μM) in the presented experiments, together with its low corrosion rate (half-life about 50 d at pH 8.7–9.2, data not shown), its concentration can be considered as constant. The slope of the regression line in Fig. 3 yields the following rate coefficients: $k_{obs} = 3.9 \times 10^{-2}\ h^{-1}$ and $k_M = 7.8 \times 10^{-3}$ L/(g_{RNIP} h) = 3.25×10^{-4} L/(m^2 h). This value is very close to the normalised (second-order) rate coefficients measured in Liu and Lowry [43], $k_M = 7 \times 10^{-3}$ L/(g_{RNIP} h), and in the same order of magnitude as derived from Tang's data [40] for another type of nZVI, $k_M \approx 2 \times 10^{-3}$ L/(g_{nZVI} h). Fig. 2 presents data derived from TCE disappearance and product formation. It is evident that the sum of the formed C_2-hydrocarbons only reaches about 85 mol% of the degraded TCE. This is a known phenomenon indicating the formation of side products other than ethene and ethane (mainly C_{3+}-hydrocarbons) [45]. The corresponding first-order plot in Fig. 3 yields a similar slope than that derived from the TCE disappearance. Because of some uncertainties in the normalization procedure (to the value of $C_{\Sigma C2,max}$) for further considerations we prefer to use k-values derived from TCE disappearance. Fig. 2 also demonstrates that the TCE concentration is practically constant in the absence of the reductant RNIP.

3.2. Sorption of TCE on activated carbon

Sorption of TCE on AC in aqueous suspension was measured in a range of equilibrium concentrations of $C_{diss\ TCE}$ = 5–60 μg/L corresponding to AC loadings of $q_{TCE\ on\ AC}$ = 2–12 mg/g. This is the same range of TCE concentrations as applied in the nZVI–AC reaction slurries. The TCE sorption was fitted to the Freundlich isotherm $q = K_F \times C_{diss}^{1/n}$ resulting in the following parameters (Fig. 4): Freundlich exponent $1/n$ = 0.682 and Freundlich coefficient K_F = 75,700 $L^{0.682}\ mg^{0.318}\ kg^{-1}$.

The sorption conditions are similar to dechlorination conditions in the presence of AC. The main outputs of these sorption data for use when interpreting the results of the dechlorination experiments are the AC loading $q_{TCE} = K_F \times C_{diss\ TCE}^{1/n} \approx 6$ mg/g (=0.6 wt%) and the freely dissolved TCE fraction $X_{diss\ TCE} = V_{water}/m_{AC} \times q^{(n-1)}/K_F^n \approx 0.004$ (=0.4% of the total TCE concentration). These are initial values at the start of a reaction period; they both decrease in the course of the dechlorination. This also applies for $X_{diss\ TCE}$ because of the nonlinearity of the sorption isotherm (increasing extent of sorption with decreasing dissolved concentration). For 90% TCE conversion, the corresponding values are $q_{TCE,\ 90\%} = 0.006 \times 0.1 = 0.0006$ (=0.06 wt%) and $X_{diss\ TCE,\ 90\%} = 0.00135$ (=0.135% of the total TCE concentration).

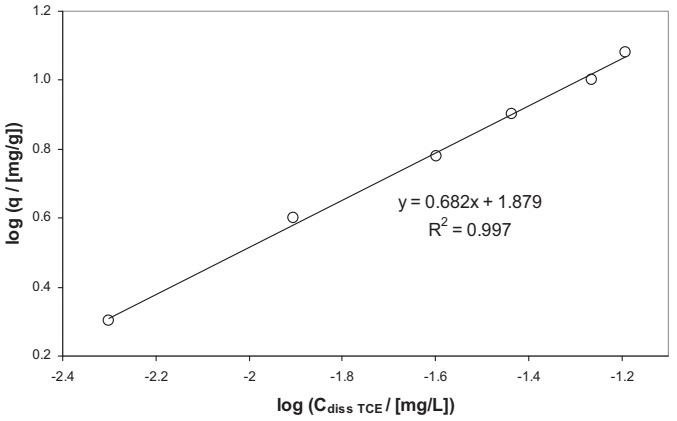

Fig. 4. Freundlich isotherm for sorption of TCE on activated carbon (SX1).

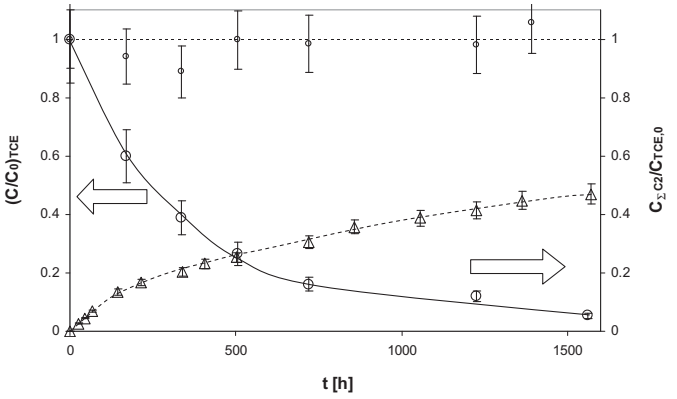

Fig. 5. Kinetics of the dechlorination of TCE with nZVI in aqueous suspension in the presence of activated carbon ($C_{TCE,0}$ = 6 mg/L, $X_{diss\ TCE} \leq 0.004$, C_{nZVI} = 5 g/L, C_{AC} = 1 g/L, 200 mM $NaHCO_3$, pH 9.0–9.8, $T = 22 \pm 2$ °C): ○ = $(C/C_0)_{TCE}$ from extract analyses (GC–MS), o = blank run without nZVI, △ = $C_{\Sigma C2}/C_{TCE,0}$ from headspace analysis (GC-FID); application of combined internal (methane) and external (methane, ethane) calibration. Error bars represent one standard deviation of single values from the mean value out of 4 replicate experiments.

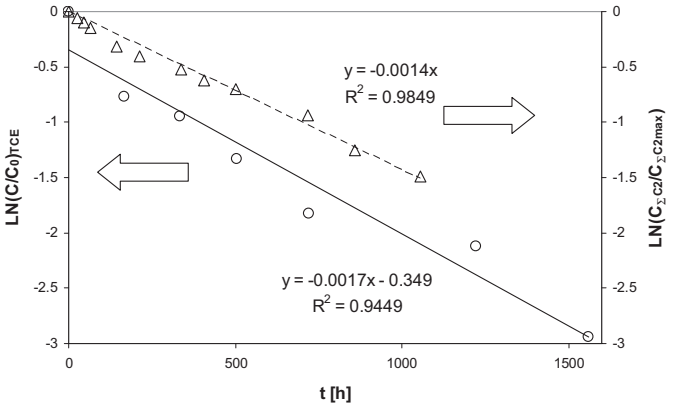

Fig. 6. Kinetics of the dechlorination of TCE with nZVI in aqueous suspension in the presence of activated carbon ($X_{diss\ TCE} \leq 0.004$): regression of data (and symbols) from Fig. 5 according to first-order reaction kinetics. C_2-product formation is normalised to a constant reaction selectivity of $C_{\Sigma C2,max}/C_{0,TCE} = 0.50$.

3.3. Dechlorination in the presence of activated carbon

When the dechlorination experiments were carried out in the presence of suspended AC (C_{AC} = 1 g/L) and otherwise applying identical reaction conditions, lower TCE rate coefficients were measured (Figs. 5 and 6): $k_{obs} = (1.4–1.7) \times 10^{-3}\ h^{-1}$ and $k_M = (2.8–3.4) \times 10^{-4}\ L/(g_{RNIP}\ h)$.

This is as can be expected due to the strong depletion of freely dissolved TCE from the aqueous solution ($X_{diss\ TCE} \leq 0.004$). The reduction in the rate coefficients amounts to a factor of $k_{TCE\ without\ AC}/k_{TCE\ with\ AC} \approx 25$. The freely dissolved TCE concentration, however, was decreased by a factor of $1/X_{diss\ TCE} \geq 250$. Obviously, the dechlorination in the presence of AC proceeds a factor of ≥10 faster than can be attributed to its freely dissolved fraction, assuming first-order reaction kinetics. In other words, more than 90% of the measured TCE conversion has to be attributed to a reaction between sorbed TCE and RNIP even though the two reactants do not come into direct contact. These conclusions apply even in the case where TCE desorption is much faster than its chemical reaction, i.e. sorption–desorption equilibria are established. Although one can suppose that some RNIP may adhere to the external surface of AC microparticles, nanoparticles ($d_{RNIP} \approx 70$ nm) definitely have no access to the micropores ($d_p \leq 2$ nm) of the AC matrix where the majority of TCE is located. Moreover, iron particles (nanoparticles and their agglomerates) and carbon particles (microparticles) can be separated by an external magnet even when they were shaken together in suspension for more than 50 d. This indicates that the majority of iron and carbon particles do not form stable mixed agglomerates. Rather they meet each other by hits and temporary contacts. Most of them are in 'dynamic contact'.

Qualitatively, this is similar to the result described by Tang et al. [40]. However, our data do not confirm their striking finding that half-lives of TCE (rate coefficients were not calculated in their study) are almost equal, independent of the presence or absence of AC. In the present study, AC does decrease the TCE reaction rate, but only by at least one order of magnitude less than it decreases the fraction of freely dissolved TCE.

3.4. Product selectivities

Product selectivities, defined as S_i = moles of product i formed from 1 mol of TCE converted, are a kind of fingerprinting of active reaction mechanisms. Therefore, they can be useful indicators for distinction between several reaction pathways. In Tang's study, ethane was the dominant dechlorination product from TCE under all reaction conditions [40]. A small fraction of ethene but no ethyne was detected. This may possibly be attributed to the high hydrogenation activity of the applied nZVI which masks the primary product distribution.

In the study of Liu et al. [46] with TCE and RNIP, all three C_2-hydrocarbons were detected. Ethyne and ethane were identified as primary products of (i) the β-elimination pathway and (ii) the hydrogenolysis + hydrogenation pathway. Ethyne was further hydrogenated to ethene. A ratio of the two rate coefficients $k_{\beta\text{-elimination}}: k_{hydrogenolysis + hydrogenation} = 5.6 \pm 1.1$ was calculated by modelling the reaction network.

In the present study, the following final product ratios were measured: with RNIP alone $S_{ethene}/S_{ethane} = 4.3 \pm 0.2$ and with the system RNIP + AC $S_{ethene}/S_{ethane} = 4.0 \pm 0.2$. The two product ratios are similar. They do not indicate different reaction sites, as could be expected for RNIP and AC surfaces as places of dechlorination reaction. A closer inspection of the initial reaction period, including ethyne as an intermediate product, yields a different pattern. Figs. 7 and 8 show results from two additional dechlorination experiments during which the headspace above the reaction slurry was analysed on a GC PLOT column where all three C_2-hydrocarbons, including ethyne, were clearly separated. The product selectivities were extrapolated here to zero-substrate conversion in order to obtain 'primary' product selectivities $S_{i,0}$, which

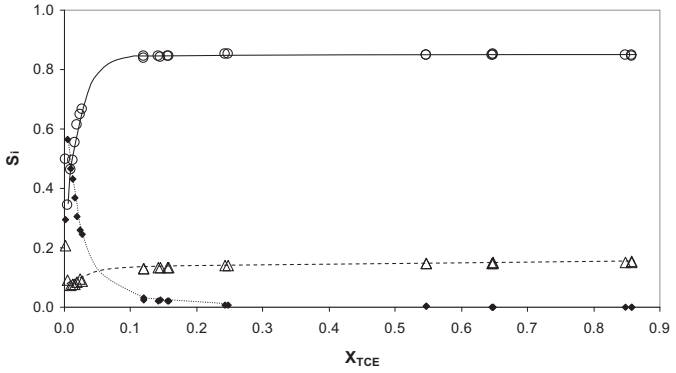

Fig. 7. Composition of the C_2-hydrocarbon fraction during dechlorination of TCE with nZVI in aqueous suspension vs. the extent of TCE conversion (X_{TCE} = 0...1 derived from C_2-formation, experimental conditions as given in Fig. 2). Selectivities S_i are normalised to the sum of $S_{ethyne} + S_{ethene} + S_{ethane} = 1.0$ ($S_i = n_i / \sum n_j$ with n = mole numbers and i, j = C_2-hydrocarbons). Legend: ♦ = ethyne, ○ = ethene, △ = ethane.

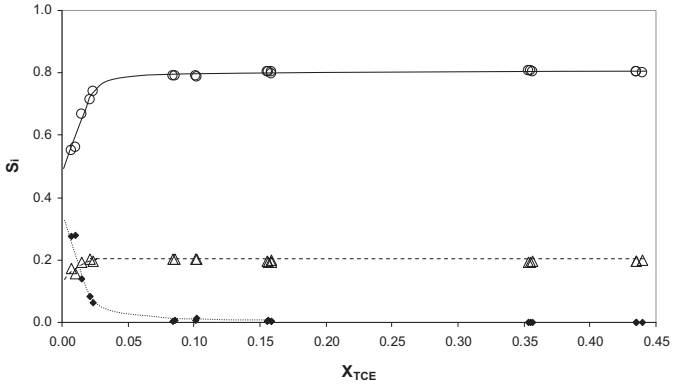

Fig. 8. Composition of the C_2-hydrocarbons during dechlorination of TCE with nZVI in aqueous suspension in the presence of activated carbon vs. the extent of TCE conversion (X_{TCE} = 0...1 derived from C_2-formation, experimental conditions as given in Fig. 5). Selectivities S_i are normalised to the sum of $S_{ethyne} + S_{ethene} + S_{ethane} = 1.0$ ($S_i = n_i / \sum n_j$ with n = mole numbers and i, j = C_2-hydrocarbons). Legend: ♦ = ethyne, ○ = ethene, △ = ethane.

are not affected by succeeding reactions. Hence, they give an unaltered image of the active reaction mechanisms.

The problem with extrapolation of product yields towards zero-substrate conversion lies in the increasing data uncertainty with decreasing extent of conversion. Nevertheless, one can extrapolate to the following primary product selectivities: (i) with RNIP only: $S_{ethyne,0}/S_{ethene,0}/S_{ethane,0}$ = 0.6/0.3/0.1 and (ii) in the presence of AC: $S_{ethyne,0}/S_{ethene,0}/S_{ethane,0}$ = 0.35/0.5/0.15. All three C_2-hydrocarbons are real primary products of TCE dechlorination. Their ratios are similar in the presence and absence of AC, with a significant shift towards hydrogenated products in the presence of AC. Summarizing these data, one can conclude that the basic reaction mechanisms of TCE dechlorination, including reductive β-elimination, hydrogenolysis, and hydrogenation seem to be the same at iron and carbon surfaces. This implies that not only electrons but also reactive hydrogen species are available at the inner surface of AC, as is also the case for the iron surface. However, it cannot be distinguished yet between hydrogen species transferred from the iron to the carbon surface (spillover) and those which are freshly generated at the carbon surface according to $H^+ + e^- \rightarrow H^*$ or $H_2O + e^- \rightarrow H^* + OH^-$ (Volmer reaction).

The sum of C_2-yields (moles of C_2-hydrocarbons per mole of TCE converted) from TCE in the presence of AC amounts to about 50% (Fig. 5). Although under long-term reaction conditions ($t_{reaction}$ up

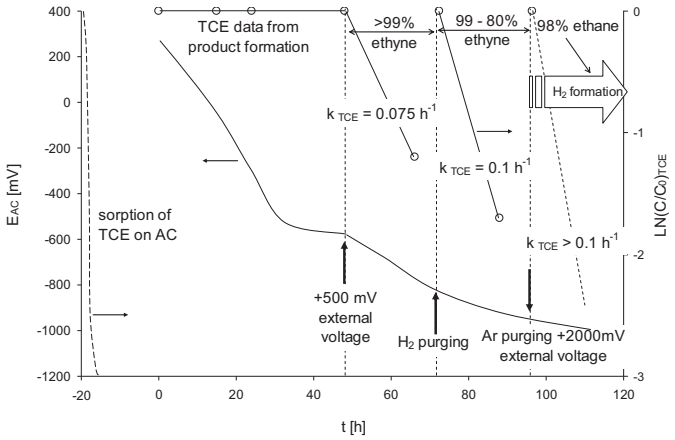

Fig. 9. Multistep experiment on electrochemical dechlorination of TCE sorbed on an AC cloth.

to 1600 h) gas-phase leakage effects (due to hydrogen formation from iron corrosion) may play a significant role and cause some uncertainties in the mass balances, the difference to pure RNIP (85%) seems to be significant. This means that dechlorination on the carbon surface gives rise to more (nonchlorinated) byproducts (C_{3+}) than are formed on the iron surface [45]. This tendency is plausible taking into account a longer residence time and a higher coverage of reactive intermediates on the carbon surface compared with the iron surface. A faster desorption of intermediates and reactive products such as ethyne tends to result in increased yields of C_2-hydrocarbons.

3.5. Electrochemical experiments

In batch suspension experiments, where ZVI and AC particles are in close contact, it is difficult to distinguish between the various transfer mechanisms—transfer of electrons or hydrogen species. In order to make this distinction, we used an electrochemical cell, where the ZVI and the AC are spatially separated but electrically connected (Fig. 1). The μZVI was placed into the anode compartment separated by a glass frit from an AC cloth which was placed into the stirred cathode compartment. The electrical resistance of the AC cloth was measured as about 100 Ω per 10 mm distance in the dry and wet state. This conductivity gives rise to a largely uniform potential across the entire cloth surface at the applied electrical currents (<1 mA)—taking into account the continuous contacting of the cloth by a thin tungsten wire. Typically we measured electron flows from 100 to 500 μA. Only part of this was actually used for chemical reactions. A major part is consumed for polarization and charging of the AC cathode, which acts as a capacitor due to its large inner surface area. The TCE (1 mg) and the internal standard methane were added to the cathode compartment and adsorbed for >24 h ($X_{TCE\ sorbed} > 0.99$). Measured TCE data are presented in Fig. 9 (broken line).

When the circuit (contactor no. 1 in Fig. 1) is closed (t = 0), an electric current flows and the AC becomes negatively charged. The course of chemical reactions was monitored by means of headspace analyses (H_2 by GC-TCD, C_2-hydrocarbons by GC-FID, chlorinated compounds by GC–MS). No hydrogen formation and no dechlorination of TCE were observed under these conditions ($X_{TCE\ converted} < 10^{-3}$, deduced from the non-detection of reaction products). The electrical current (decreasing from 600 to 100 μA within 48 h) is attributed to iron corrosion and charging of the AC capacitor. After 48 h an external electrical voltage of 500 mV was applied (contactor no. 1 open). Within the next 24 h about 80% of

the sorbed TCE was decomposed. The $LN(C/C_0)_{TCE}$ plots in Fig. 9 for all the reaction periods were calculated from product formation ($LN(1 - C_{\Sigma C2}/C_{\Sigma C2max})$) rather than TCE depletion because the TCE concentration profiles were affected by superposition of sorption and reaction kinetics after respiking of fresh TCE. The main products were ethyne (with only traces of ethene and no ethane) and partially dechlorinated products, mainly *cis*-DCE and VC. After purging the cell with H_2 (instead of Ar) and respiking with 1 mg of TCE (t = 72 h), dechlorination continues with ethyne as the only primary C_2-hydrocarbon. Some slow hydrogenation yielding ethene and ethane was observed (20% and 3%, respectively, of the C_2-fraction after t = 96 h). Hydrogenation was clearly identified as a successive reaction rather than as a parallel dechlorination pathway. The extent of partial dechlorination was not significantly decreased by the hydrogen atmosphere. The dechlorination proceeded slightly faster in the presence of H_2, but this may be due to the continuously decreasing cathode potential. Obviously, the molecular hydrogen (H_2) is not efficiently involved in the primary dechlorination reactions. These can be interpreted as stepwise electron transfer giving rise to reductive β-elimination (ethyne formation) and stepwise hydrogenolysis of C—Cl-bonds (DCE formation).

After t = 96 h the cathode compartment was purged with Ar to remove the hydrogen completely and respiked again with 1 mg of TCE. The external voltage was increased to 2000 mV. Under these conditions, hydrogen was generated at the cathode by water electrolysis. The TCE was completely converted after 24 h. Ethane was the main product with only 2% ethene and no ethyne. No partially dechlorinated products were detected.

Obviously, the availability of surface-bound nascent hydrogen species H* on the AC surface shifts the dechlorination mechanism significantly from electron-transfer to hydrogenation. When only electrons are available as reducing species (t = 48–96 h), ethyne and *cis*-DCE are the dominant products from TCE. When active H* species are amply available (t = 96–112 h), total dechlorination and hydrogenation prevail. Comparing these characteristic product patterns with those observed in the nZVI–AC-slurry experiments (e.g. ethane as a primary product), one can conclude that not only electrons but also H* species are amply available at the inner surface of AC particles. We could also demonstrate that molecular hydrogen, which is always formed in aqueous ZVI slurries, is not able to play a similar role. The described electrochemical findings enable a distinction to be made between the two possible sources of surface hydrogen species: (i) H-spillover from the ZVI surface to the AC particles [48,49], and (ii) the electrochemical generation of H* inside the AC pores. In addition, there is another argument against a dominant role of the electrochemical pathway: carbon surfaces expose a higher overpotential for hydrogen generation compared with iron surfaces (about 300–500 mV more negative on carbon [56]). This overpotential is mainly caused by an electron throughput barrier [57] which makes the iron surface a more efficient place of hydrogen generation than the carbon surface. There is no reason for electrons to move from an iron surface to a carbon surface in order to reduce protons under less favourable conditions there.

The described electrochemical experiments were designed to give more insight into the reaction mechanisms under different reaction conditions. The bare 'electrical contact' between a static μZVI layer and the AC cloth did not give rise to any TCE conversion. Obviously, these conditions are different from those in an agitated mixed slurry, where the particles come in direct and dynamic contact and TCE reduction occurs. Note that no hydrogen transfer is possible under the static conditions because iron and AC are spatially separated. When the AC potential is further decreased by means of an external voltage supply, a fast TCE dechlorination is initiated. The estimated first-order rate coefficients of the electrochemical TCE dechlorination are two orders of magnitude higher than in the slurry reactor ($k_{TCE\ sorbed} \approx 0.1\ h^{-1}$ vs. $0.0015\ h^{-1}$).

4. Conclusions

4.1. Implications of the present findings

Activated carbon as an excellent sorbent of many organic compounds, and nZVI as an environmentally friendly reductant can cooperate in such a way that the reducing power of iron particles is transferred onto the carbon matrix. A chemical reaction does not presuppose the direct contact between the sorbate and the iron surface. This may provide further information regarding the mode of action of the two elements in the Carbo-Iron™ remediation reagent [34–36]. Our experiments show that carbon surfaces can function as true catalyst for the reductive dechlorination of TCE. Note that the phenomenon described here differs from several other studies discussing the role of carbonaceous materials as catalysts in reduction reactions [50–52], where the reductants are in the dissolved state having free access to sorbed pollutants and reaction sites: the particulate reductant nZVI does not have access into the AC pores.

4.2. Mechanistic interpretation

Our results are in principal conformity with those from Chen's study [40] and complement them with respect to particle size, initial AC loadings, pH range and fingerprinting of primary reaction products. The presented data are one of the very few cases where a spillover-like phenomenon is described for an aqueous system [48,49,53–55]. The spillover mechanism decouples the transport of electrons and hydrogen species across particles and surfaces, implying a long-range migration of H*. The electrochemical experiment proves that the bare electrical contact between ZVI and AC, giving rise to electron transport, is not sufficient for TCE dechlorination inside the AC pores. Lower reduction potentials can initiate TCE reduction, but with a significantly altered product pattern (ethyne + *cis*-DCE as major products). It is only in the presence of nascent hydrogen that the product pattern typical of dechlorination on ZVI is also obtained on AC (ethene + ethane as major products).

Very recently, Xu et al. [58] have investigated the interplay between sorption and reaction with a number of halogenated and nitrated compounds adsorbed on black carbon with sulphide as reductant. They found that only nitrated compounds were reduced under the applied conditions, whereas halogenated compounds were not. The reduction takes place via electron transfer directly from sorbed sulphides rather than via transfer of electrons through conductive carbon regions. Obviously, sulphide–carbon and iron–carbon systems behave differently with respect to the transfer mechanisms.

In order to further exploit the potential of iron-carbon mixtures for remediation purposes, it is necessary to investigate whether and for how long iron particles can transfer reactive species (electrons and/or hydrogen species) onto the carbon matrix without any agitation, i.e. in a static fixed bed. In addition, it is of interest to check whether the described spillover phenomenon is specific to nanoparticles or whether it can also be observed for larger particles. Studies to answer these questions are currently in progress.

Acknowledgements

The authors thank the graduate schools BuildMoNa at Leipzig University and HIGRADE at the UFZ, as well as the BMBF (German Federal Ministry of Education and Research) for financial support within the project Fe-NANOSIT. They also thank Mrs. K. Lehmann for technical assistance in the experimental part.

Appendix A. Supplementary data

Supplementary data associated with this article can be found, in the online version, at http://dx.doi.org/10.1016/j.apcatb.2015.08.031.

References

[1] R.W. Gillham, S.F. O'Hannesin, Ground Water 32 (1994) 958–967.
[2] L.J. Matheson, P.G. Tratnyek, Environ. Sci. Technol. 28 (1994) 2045–2053.
[3] F. Fu, D.D. Dionysiou, H. Liu, J. Hazard. Mater. 267 (2014) 194–205.
[4] C.-B. Wang, W.-X. Zhang, Environ. Sci. Technol. 31 (1997) 2154–2156.
[5] W.-X. Zhang, C.-B. Wang, Catal. Today 49 (1998) 387–395.
[6] W.-X. Zhang, J. Nanopart. Res. 5 (2003) 323–332.
[7] F.-D. Kopinke, A. Georgi, H. Weiß, J. Nanopart. Res. 6 (2004) 123.
[8] W.-X. Zhang, D.W. Elliott, Rem. J. 16 (2006) 7–21.
[9] L. Li, M. Fan, R.C. Brown, J. Van Leeuwen, J. Wang, W. Wang, Y. Song, P. Zhang, Crit. Rev. Environ. Sci. Technol. 36 (2006) 405–431.
[10] R. Koeber, F.-D. Kopinke, TerraTech 16 (6) (2007) 17–20.
[11] N. Mueller, J. Braun, J. Bruns, M. Černík, P. Rissing, D. Rickerby, B. Nowack, Environ. Sci. Pollut. Res. 19 (2012) 550–558.
[12] W. Yan, H.-L. Lien, B.E. Koel, W.-X. Zhang, Environ. Sci. Proc. Impacts 15 (2013) 63–77.
[13] T. Tosco, M.P. Papini, C.C. Vigg, R. Sethi, J. Clean. Prod. 77 (2014) 10–21.
[14] R.A. Crane, T.B. Scott, J. Hazard. Mater. 211–212 (2012) 112–125.
[15] D.R. Burries, T.J. Campbell, V.S. Manoranjan, Environ. Sci. Technol. 29 (1995) 2850–2855.
[16] R.M. Allen-King, R.M. Halkert, D.R. Burris, Environ. Toxicol. Chem. 16 (1997) 424–429.
[17] D.R. Burris, R.M. Allen-King, V.S. Manoranjan, T.J. Campbell, G.A. Loraine, B. Deng, J. Environ. Eng. ASCE 124 (1998) 1012–1019.
[18] J. Dries, L. Bastiaens, D. Springael, S.N. Agathos, L. Diels, Environ. Sci. Technol. 38 (2004) 2879–2884.
[19] H. Zhang, Z.-H. Jin, L. Han, C.-H. Qin, Trans. Nonferrous Met. Soc. 16 (2006) s345–s349.
[20] L.B. Hoch, E.J. Mack, B.W. Hydutsky, J.M. Hershman, J.M. Skluzacek, T.E. Mallouk, Environ. Sci. Technol. 42 (2008) 2600–2605.
[21] H. Cao, G. Huang, S. Xuan, Q. Wu, F. Gu, C. Li, J. Alloys Compd. 448 (2008) 272–276.
[22] H. Choi, S.R. Al-Abed, S. Agarwal, D.D. Dionysiou, Chem. Mater. 20 (2008) 3649–3655.
[23] H. Zhu, Y. Jia, X. Wu, H. Wang, J. Hazard. Mater. 172 (2009) 1591–1596.
[24] H. Choi, S. Agarwal, S.R. Al-Abed, Environ. Sci. Technol. 43 (2009) 488–493.
[25] M.C. Pereira, F.S. Coelho, C.C. Nascentes, J.D. Fabris, M.H. Araújo, K. Sapag, L.C.A. Oliveira, R.M. Lago, Chemosphere 81 (2010) 7–12.
[26] Z. Liu, F.-S. Zhang, Bioresour. Technol. 101 (2010) 2562–2564.
[27] B. Sunkara, J. Zhan, J. He, G.L. McPherson, G. Piringer, V.T. John, ACS Appl. Mater. Interfaces 2 (2010) 2854–2862.
[28] J. Zhan, I. Kolesnichenko, B. Sunkara, J. He, G.L. McPherson, G. Piringer, V.T. John, Environ. Sci. Technol. 45 (2011) 1949–1954.
[29] H. Sun, G. Zhou, H.M. Ang, M.O. Tade, S. Wang, Appl. Mat. Interfaces 4 (2012) 6235–6241.
[30] S.J. Lee, J. Jung, M.A. Kim, Y.-R. Kim, J.K. Park, J. Mater. Sci. 47 (2012) 8112–8117.
[31] H. Fu, Y. Guo, W. Chen, C. Gu, D. Zhu, Carbon 72 (2014) 74–81.
[32] K. Mackenzie, A. Schierz, A. Georgi, F.-D. Kopinke, Global NEST J. 10 (2008) 54–61.
[33] K. Mackenzie, S. Bleyl, F.-D. Kopinke, Water Res. 46 (2012) 3817–3826.
[34] S. Bleyl, K. Mackenzie, F.-D. Kopinke, Chem. Eng. J. 191 (2012) 588–595.
[35] K. Mackenzie, S. Bleyl, A. Schierz, A. Georgi, Nanotechnology for Water Treatment, Universal Publishers, Boca Raton, USA, 2012, 46 ff.
[36] S. Bleyl, F.-D. Kopinke, K. Mackenzie, Chem. Ing. Tech. 85 (2013) 1–11.
[37] http://www.nanorem.eu
[38] http://www.nanopartikel.info/projekte/abgeschlossene-projekte/fe-nanosit
[39] A. Georgi, F.-D. Kopinke, Appl. Catal. B: Environ. 58 (2005) 9–18.
[40] H. Tang, D. Zhu, T. Li, H. Kong, W. Chen, J. Environ. Qual. 40 (2011) 1878–1885.
[41] S.Y. Oh, D.K. Cha, P.C. Chiu, Environ. Sci. Technol. 36 (2002) 2178–2184.
[42] J.C. Ye, P.C. Chiu, Environ. Sci. Technol. 40 (2006) 3959–3964.
[43] Y. Liu, G.V. Lowry, Environ. Sci. Technol. 40 (2006) 6085–6090.
[44] G. Ertl, et al., Handbook of Heterogeneous Catalysis, vol. 5, Wiley-VCH, Weinheim, 2008, Chapter 5.2.3., 1482 ff.
[45] W.A. Arnold, A.L. Roberts, Environ. Sci. Technol. 34 (2000) 1794–1805.
[46] Y. Liu, S.A. Majetich, R.D. Tilton, D.S. Sholl, G.V. Lowry, Environ. Sci. Technol. 39 (2005) 1338–1345.
[47] Y. Liu, T. Phenrat, G.V. Lowry, Environ. Sci. Technol. 41 (2007) 7881–7887.
[48] W.C. Conner, J.L. Falconer, Chem. Rev. 95 (1995) 759–788.
[49] R. Prins, Chem. Rev. 112 (2012) 2714–2738.
[50] J.M. Kemper, E. Ammar, W.A. Mitch, Environ. Sci. Technol. 42 (2008) 2118–2123.
[51] H. Fu, D. Zhu, Environ. Sci. Technol. 47 (2013) 4204–4210.
[52] H. Fu, Y. Guo, W. Chen, C. Gu, D. Zhu, Carbon 72 (2014) 74–81.
[53] C. Amorim, M.A. Keane, J. Colloid Interface Sci. 322 (2008) 196–208.
[54] C. Amorim, M.A. Keane, J. Hazard. Mater. 211–212 (2012) 208–217.
[55] O.M. Ilinich, E.N. Gribov, P.A. Simonov, Catal. Today 82 (2003) 49–56.
[56] K.J. Vetter, Elektrochemische Kinetik, Springer-Verlag, Berlin Goettingen Heidelberg, 1961, p. 432.
[57] P. Drossbach, J. Schulz, Electrochim. Acta 9 (1964) 1391–1404.
[58] W. Xu, J.J. Pignatello, W.A. Mitch, Environ. Sci. Technol. 49 (2015) 3419–3426.